ARL-TR-95-11

Copy No. 23

Analysis of Sea Test Data I

Final Report under Contract N00039-91-C-0082
TD No. 01A2059, Analysis of Sea Test Data I

Nicholas P. Chotiros

Applied Research Laboratories
The University of Texas at Austin
P. O. Box 8029 Austin, TX 78713-8029

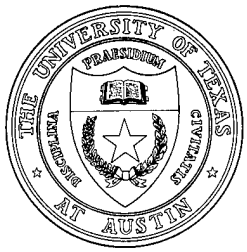

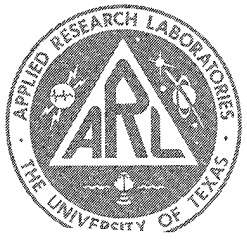

20 April 1995

Final Repo

3 March 1993 - 28 F

Approved for public release;
distribution is unlimited.

Prepared for:
Naval Research Laboratory
Stennis Space Center, MS 39529-5004

Monitored by:
Space and Naval Warfare Systems Command
Department of the Navy
Arlington, VA 22245-5200

REPORT DOCUMENTATION PAGE

Form Approved
OMB No. 0704-0188

1. AGENCY USE ONLY (Leave blank)	2. REPORT DATE	3. REPORT TYPE AND DATES COVERED
	20 Apr 95	final 3 Mar 93 - 28 Feb 95

4. TITLE AND SUBTITLE
Analysis of Sea Test Data I, Final Report under Contract N00039-91-C-0082, TD No. 01A2059, Analysis of Sea Test Data I

5. FUNDING NUMBERS
N00039-91-C-0082,
TD No. 01A2059

6. AUTHOR(S)
Chotiros, Nicholas P.

7. PERFORMING ORGANIZATION NAMES(S) AND ADDRESS(ES)
Applied Research Laboratories
The University of Texas at Austin
P.O. Box 8029
Austin, Texas 78713-8029

8. PERFORMING ORGANIZATION REPORT NUMBER
ARL-TR-95-11

9. SPONSORING/MONITORING AGENCY NAME(S) AND ADDRESS(ES)
Naval Research Laboratory
Stennis Space Center, MS 39529-5004

Space and Naval Warfare
Systems Command
Department of the Navy
Arlington, VA 22245-5200

10. SPONSORING/MONITORING AGENCY REPORT NUMBER
NRL/CR/7170--96-0005

11. SUPPLEMENTARY NOTES

12a. DISTRIBUTION/AVAILABILITY STATEMENT
Approved for public release; distribution is unlimited.

12b. DISTRIBUTION CODE

13. ABSTRACT (Maximum 200 words)
Sound propagation from water into the sediment was analyzed specifically to test the validity of Biot's theory at high frequencies. Two acoustic waves were detected in sand as predicted by the theory. Measurements were made in both muddy and sandy sediments. Experiments were conducted by NRL/SSC in cooperation with ARL:UT in a muddy sediment in Eckernförde, Germany, and in a sandy sediment off Panama City, Florida. Carrier frequencies used were 20, 40, 60, 90, 110, 131, 150, and 179 kHz. Anomalies in the measured sound pressure as a function of depth prevented the estimation of absorption coefficients at the lower frequencies.

14. SUBJECT TERMS
acoustic, attenuation, Biot, mud, penetration, sand, sediment, speed

15. NUMBER OF PAGES
31

16. PRICE CODE

17. SECURITY CLASSIFICATION OF REPORT	18. SECURITY CLASSIFICATION OF THIS PAGE	19. SECURITY CLASSIFICATION OF ABSTRACT	20. LIMITATION OF ABSTRACT
UNCLASSIFIED	UNCLASSIFIED	UNCLASSIFIED	SAR

NSN 7540-01-280-5500

Standard Form 298 (Rev. 2-89)
Prescribed by ANSI Std. 239-18
298-102

This page intentionally left blank.

TABLE OF CONTENTS

This page intentionally left blank.

LIST OF FIGURES

This page intentionally left blank.

PREFACE

This report is the final report on the work ARL:UT was tasked to do under Contact N00039-91-C-0082, TD No. 01A2059, "Analysis of Sea Test Data I".

This page intentionally left blank.

1. INTRODUCTION

Experiments were conducted by Naval Research Laboratory/Stennis Space Center (NRL/SSC) in cooperation with Applied Research Laboratories, The University of Texas at Austin (ARL:UT), to measure sound propagation at two sites, in a muddy sediment at Eckernförde, Germany, and in a sandy sediment off Panama City, Florida. The objective was to study the sound propagating from water into the sediment, in particular, to test the validity of Biot's theory at high frequencies, as part of the Coastal Benthic Boundary Layer Special Research Program (CBBL SRP). The data collected were analyzed by ARL:UT for sound propagation through the sediment. A sparse array buried in the sediment was used to collect the acoustic data. It was designed to detect acoustic waves traveling at speeds in the range of 600-2000 m/s. Based on previous experience, this range is expected to encompass all of the acoustic waves that may be present in unconsolidated shallow water sediments. A sharp contrast was expected between the results from the soft muddy sediment and from the harder sandy sediment. The acoustic data are particularly valuable because they are supported by environmental measurements by other CBBL participants, including depth sounder and sidescan sonar data, and extensive core samples throughout the test area. This report describes the methods used to detect and measure the direction and speed of acoustic waves and their attenuations, and the results obtained.

This page intentionally left blank.

2. EXPERIMENT

Based on previous experimental results and knowledge of the geophysics of sandy sediments, a model of acoustic sediment penetration was constructed. The model was used to estimate the penetration of acoustic waves at frequencies in the high frequency band. Based on these results, a hydrophone array was designed to detect and measure the speed and attenuation of sediment penetrating waves.

A set of acoustic projectors was mounted on a tower at a height of approximately 7 m above the bottom. Hydrophone arrays were planted in the sediments. Each array consisted of four hydrophones: one on the sediment surface and two others directly beneath. The fourth hydrophone was planted down range. The configuration of the array used in the muddy site is as shown in Fig. 2.1. The deepest hydrophone was at a depth of 0.732 m, and connected to receiver channel 33. The second deepest was at a depth of 0.518 m, and connected to channel 34. The down range hydrophone was connected to channel 35. The surface hydrophone was connected to channel 36. The array configuration in the sandy site is shown in Fig. 2.2. The deepest hydrophone was at 0.30 m, and connected to channel 34. The depths and receiver channels are as shown in Fig. 2.2. At both sites, three hydrophone arrays were deployed at ranges of 13.7, 20.1, and 39.4 m from the projector, giving grazing angles of 30°, 18°, and 10°, as shown in Fig. 2.3.

Signals were transmitted from the projector to the hydrophones. Carrier frequencies used were 20, 40, 60, 90, 110, 131, 150, and 179 kHz. In all cases, the received signals were amplified, demodulated to a center frequency of 5 kHz and low pass filtered at 10 kHz, sampled at 20 kHz, and digitized to optical disk, by NRL/SSC, under the direction of Dr. Steve Stanic.

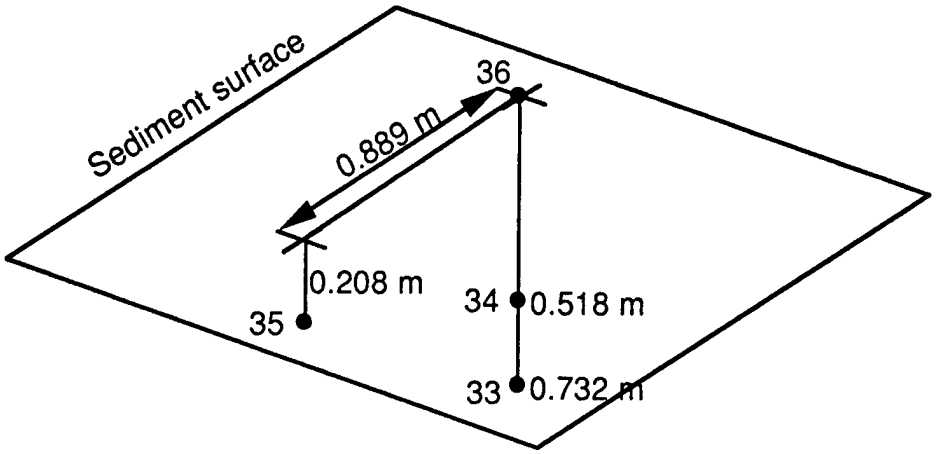

Figure 2.1
Buried hydrophone array: muddy site.

ARL:UT
AS-95-627
NPC - rfg
9-95

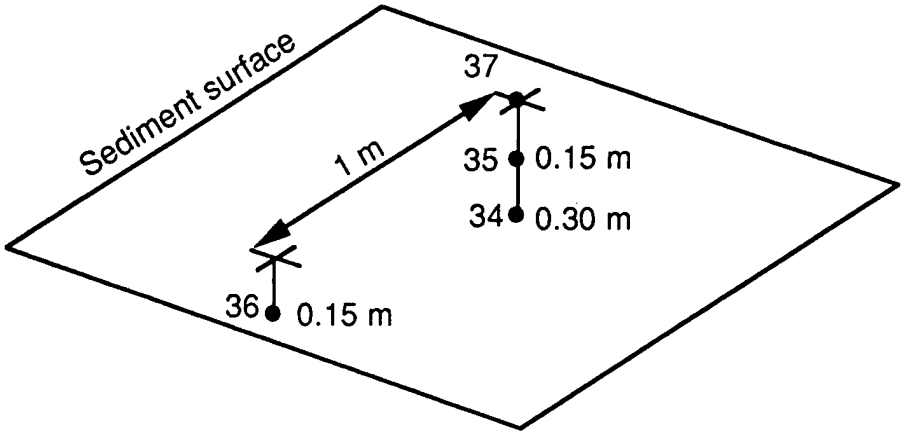

Figure 2.2
Buried hydrophone array: sandy site.

ARL:UT
AS-95-628
NPC - rfg
9-95

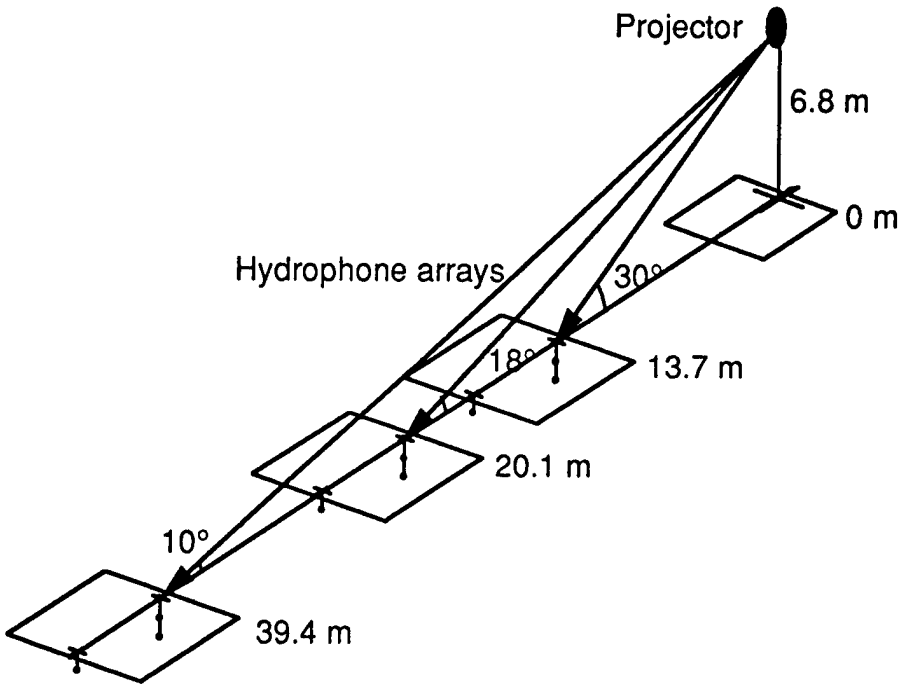

Figure 2.3
Layout of hydrophone arrays and projector.

ARL:UT
AS-95-629
NPC - rfg
9-95

3. DATA PROCESSING

3.1 PULSE COMPRESSION

The pulses used were typically cw or linear frequency modulation (LFM) chirp pulses of a duration of 0.5 - 5 ms. The recorded data were generally of good quality. Those at the higher frequencies tended to be contaminated by system noise to some degree. An example of the received signals at 110 kHz, from run 313 of the sandy site, at the shortest range, is shown in Fig. 3.1. Two signals are shown. The signal from channel 37 is from the surface hydrophone, and that from channel 36 is from the buried hydrophone 1 m down range. The signals from the buried hydrophones, such as channel 36, tend to be weaker, hence more noisy.

In computing wave direction and speed, it is necessary to be able to accurately resolve the arrival time differences of the signals at the four hydrophones. Normally, phase coherent methods are the most sensitive. However, in an experiment of this type, the placement of the hydrophones will have an error that is typically larger than the signal wavelength at these frequencies. Therefore, phase information is not expected to be usable.

Without phase information, the next best approach is to compress the pulse and resolve arrival times with the compressed signal envelope. The usable signal bandwidth is approximately 5 kHz, which should be able to provide a pulse width, hence timing resolution, of 0.2 ms. The signal in channel 37, the surface hydrophone, was used as the reference signal; the time of its arrival is defined as t=0. Its fast Fourier transform (FFT) was used to construct a bandlimited inverse filter, which is applied to the signals from all four hydrophones. The filtered signals were coherently averaged over a number of pings. Corresponding examples of the resulting signal envelopes squared are shown in Fig. 3.2. In this example, the filtered signals were averaged over ten pings. A pulse width of 0.2 ms was achieved. Furthermore, the improved signal-to-noise ratio (SNR) permits a timing resolution significantly better than the pulse width.

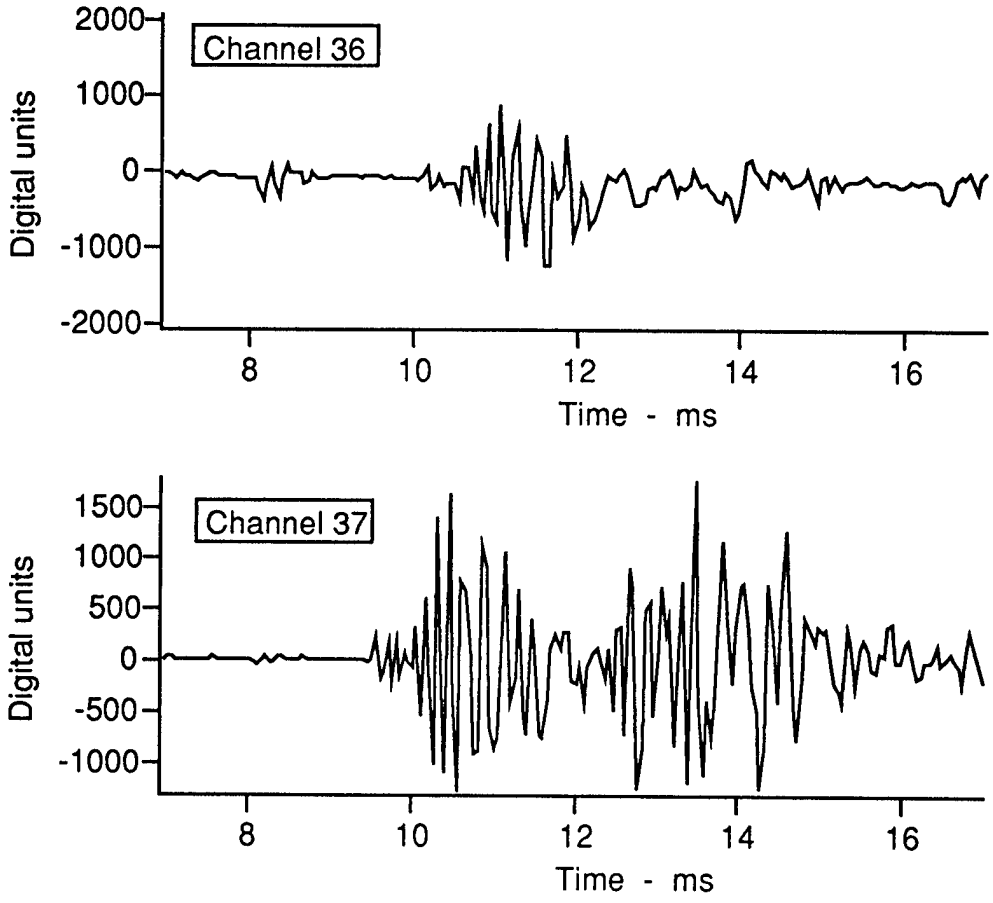

Figure 3.1
Examples of raw signal pulses.

ARL:UT
AS-95-630
NPC - rfg
9-95

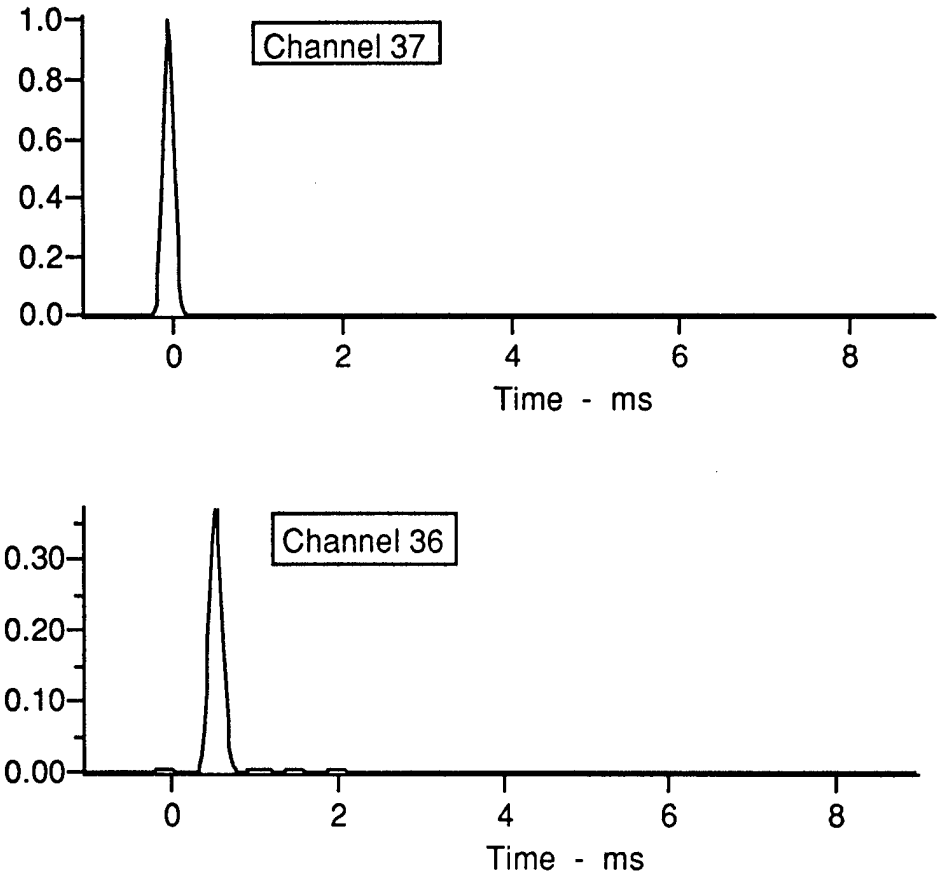

Figure 3.2
Examples of compressed signal pulse envelopes squared.

ARL:UT
AS-95-631
NPC - rfg
9-95

3.2 WAVE SPEED AND DIRECTION

Using a simple linear superposition method, a plot of relative intensity of acoustic waves, as a function of speed and direction, was generated for each run. The output is in the form of an intensity plot in a direction-speed space; direction is in the form of elevation angle, within the vertical section through the source position and the centroid of the hydrophone array, and ranging from +90° (upward vertical) to -90° (downward vertical); the speed range is 600-2500 m/s, in a scale that is inversely linear. A peak in intensity is indicative of a wave traveling at the indicated wave speed and direction.

The results from the sandy site are shown in Fig. 3.3. Runs 298-313 cover the frequencies of 20-110 kHz at a grazing angle of 30°. It is seen that at the low end of the spectrum, the dominant wave is the fast wave, traveling at a very slight depression angle, at a speed of approximately 1700 m/s, which is consistent with sound speeds measured from core samples by Briggs and Richardson.[1] At higher frequencies, a slow wave at a speed of 1200 m/s tends to dominate. At 110 kHz, run 313, both waves are detectable. The normalized signal envelopes are shown in Fig. 3.4(a). The signal at the deepest hydrophone, channel 34, has two discernible peaks, corresponding to the fast and slow waves, respectively. Runs 341-351 (Fig. 3.3) cover a similar range of frequencies, but at a grazing angle of 10°. In this case, the slow wave appears to be dominant at all frequencies. There is one anomalous result in run 349 at 40 kHz, where another wave, at a speed of 850 m/s, is indicated. Given the grazing angle and the sound speed in water, Snell's Law of refraction may be used to predict a curve in the direction/speed space on which all refracted waves must lie. On comparison with Snell's Law of refraction, there appears to be a constant offset in angle that suggests that the array may be slightly tilted. This is illustrated in Fig. 3.4(b) for the 30° grazing angle case, where the tilt is estimated to be -7.7°. In the 10° case, it is estimated to be +8.2°. After allowing for these angle offsets, Snell's Law of refraction is coincident with the speed and direction of both the fast and slow waves in all cases.

The results from the muddy site are shown in Fig. 3.5. Only the data from the 10° grazing angle case were analyzed. The results clearly show only one

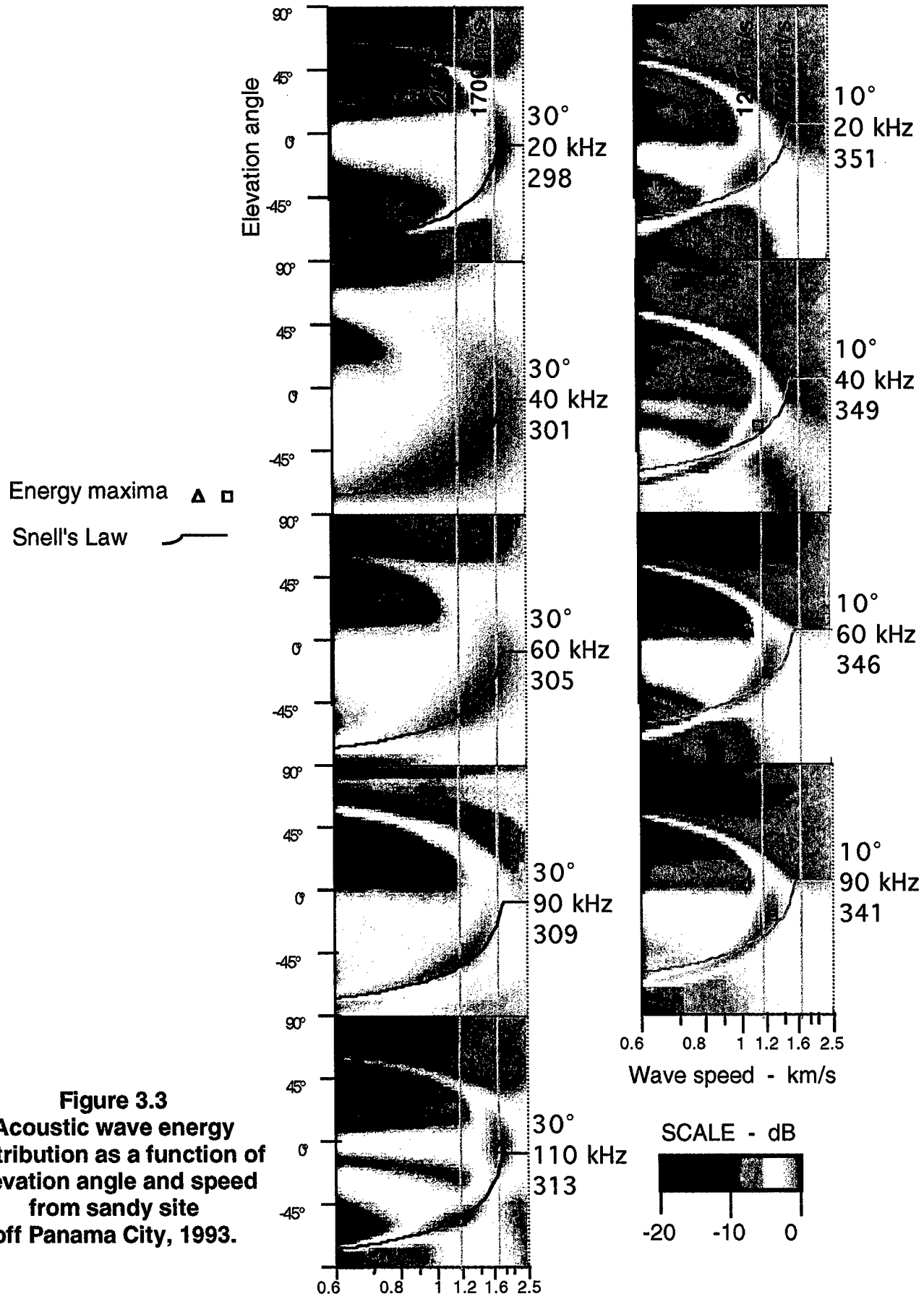

Figure 3.3
Acoustic wave energy distribution as a function of elevation angle and speed from sandy site off Panama City, 1993.

ARL:UT
AS-95-632
NPC - rfg
9-95

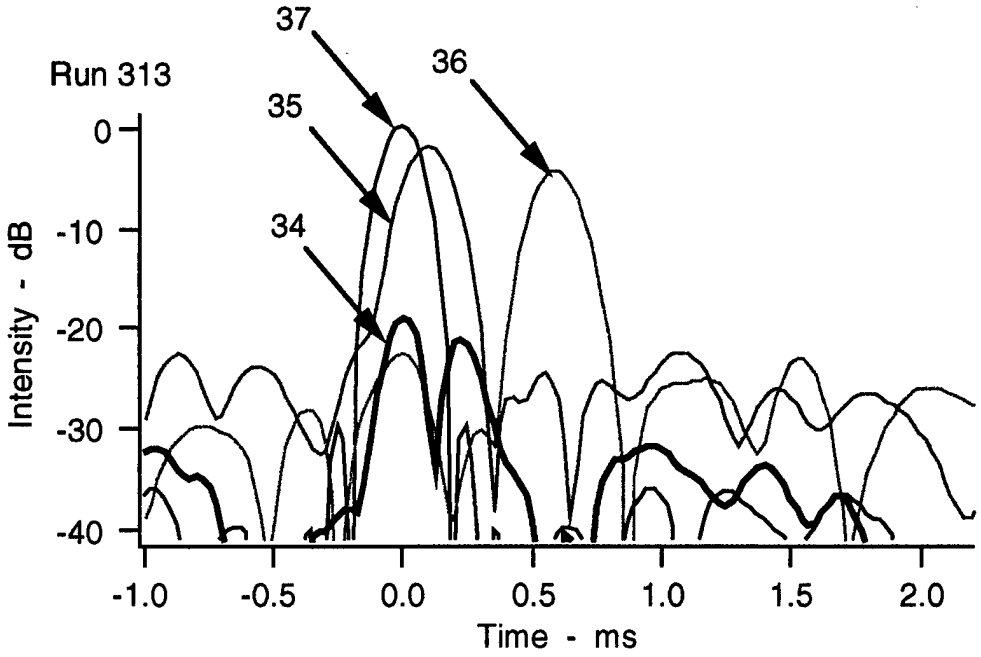

(a) Signal levels and arrival times relative to surface hydrophone

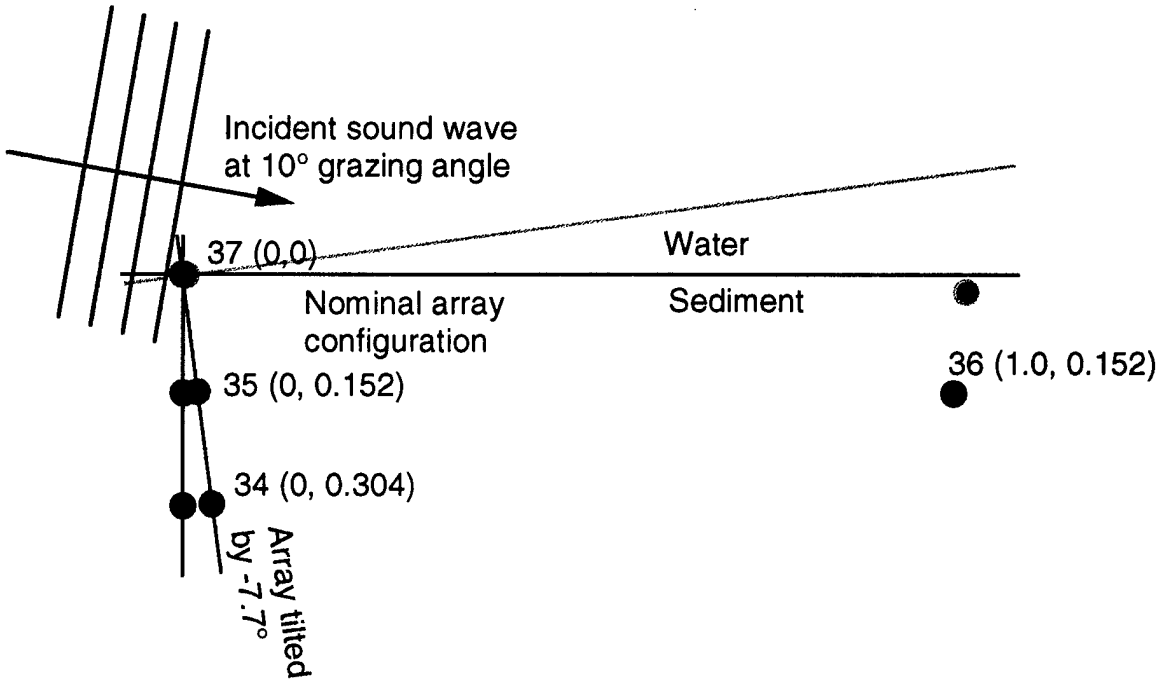

(b) Nominal array configuration and estimated array tilt angle

Figure 3.4
Sandy site, run 313, at a grazing angle of 30°.

ARL:UT
AS-95-633
NPC - rfg
9-95

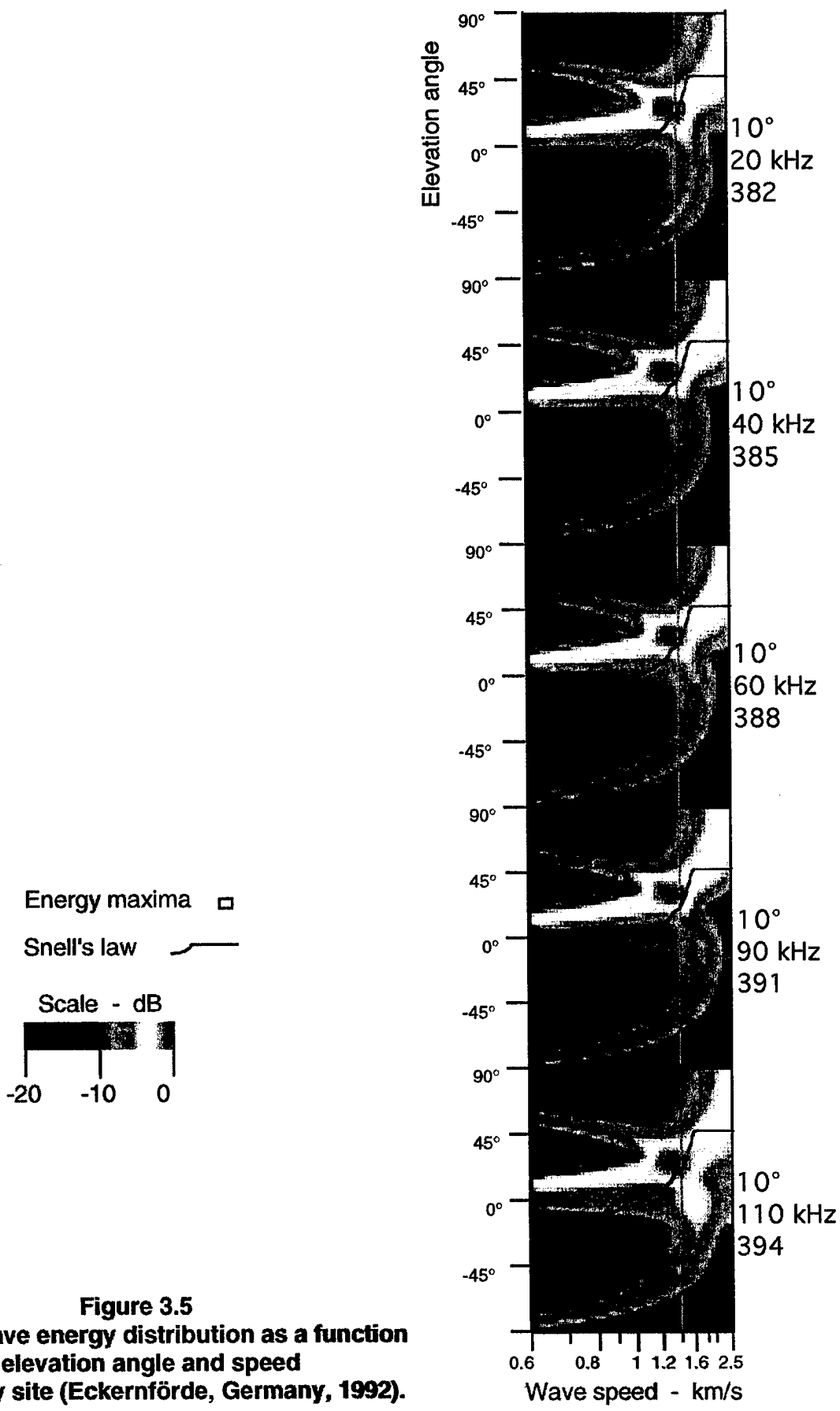

Figure 3.5
Acoustic wave energy distribution as a function of elevation angle and speed from muddy site (Eckernförde, Germany, 1992).

ARL:UT
AS-95-634
NPC - fig
9-95

acoustic wave, propagating at a speed of approximately 1400 m/s which is consistent with sound speeds measured from core samples by Briggs and Richardson.[1] The direction, however, is 30° upward relative to the horizontal. This is confirmed by the relative arrival times of the signal pulses, shown in Fig. 3.6 for run 388, which shows pulses at the deeper hydrophones arriving earlier. This could conceivably be a wave reflected from a subbottom layer but this is unlikely, because there is no sign of the direct wave, or any other wave. The most likely explanation is that the array is tilted by an angle of 45°, as illustrated in Fig. 3.6(b). When the Snell's Law of refraction curve is offset by this angle, it coincides with the direction and speed of the measured waves, as shown in Fig. 3.5. However, the array was installed with great care in its proper orientation, and the interpretation of these results remains unresolved.

3.3 WAVE ATTENUATION

The relative signal levels from the sandy site, at a grazing angle of 30°, referenced to the level at the surface hydrophone, are shown in Fig. 3.7, as a function of hydrophone depth and frequency. Except for the deepest hydrophone, there does not appear to be a monotonic decrease in signal level as a function of depth. The reason for this phenomenon is not clear. It is most likely caused by interference between the slow and fast waves, since the results in Fig. 3.3 indicate that both waves are present. This makes it impossible to make reliable estimates of attenuation coefficients. Attenuation coefficients were computed at 60 kHz where the dominant wave was the fast wave (1700 m/s), and at 110 kHz where the slow wave was dominant (1200 m/s). These results should be considered as very approximate. At a grazing angle of 10°, the signal levels are more consistent, as shown in Fig. 3.8. From wave speed and direction analysis, it was determined that only the slow wave is present. The signal levels at 20 kHz are a problem because they appear to be increasing with depth. At higher frequencies, the levels decrease with increasing depth and estimates were made of the attenuation coefficient, as shown in Table 3.1.

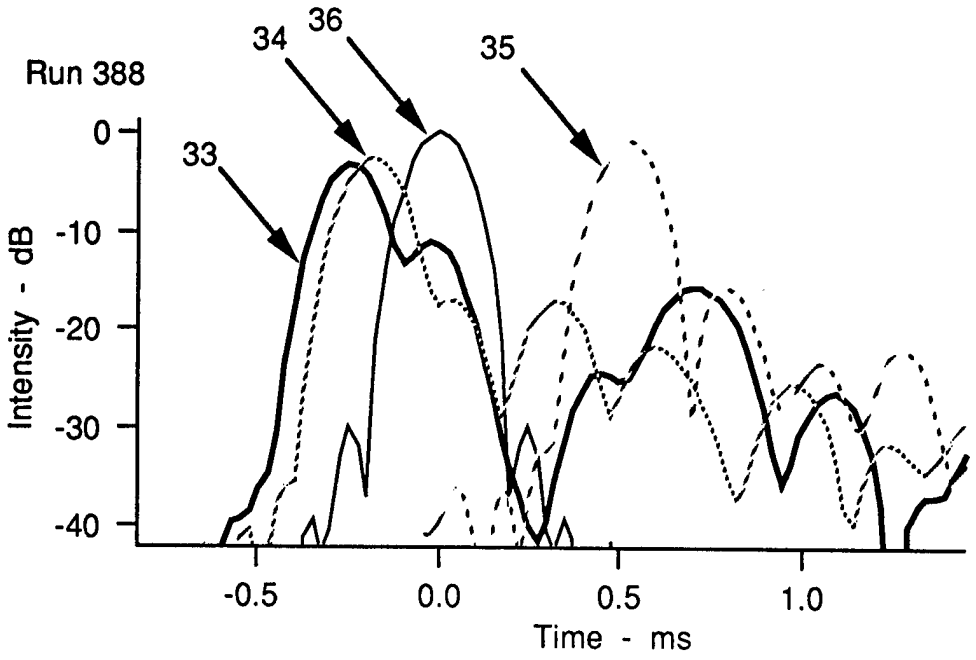

(a) Signal levels and arrival times relative to surface hydrophone

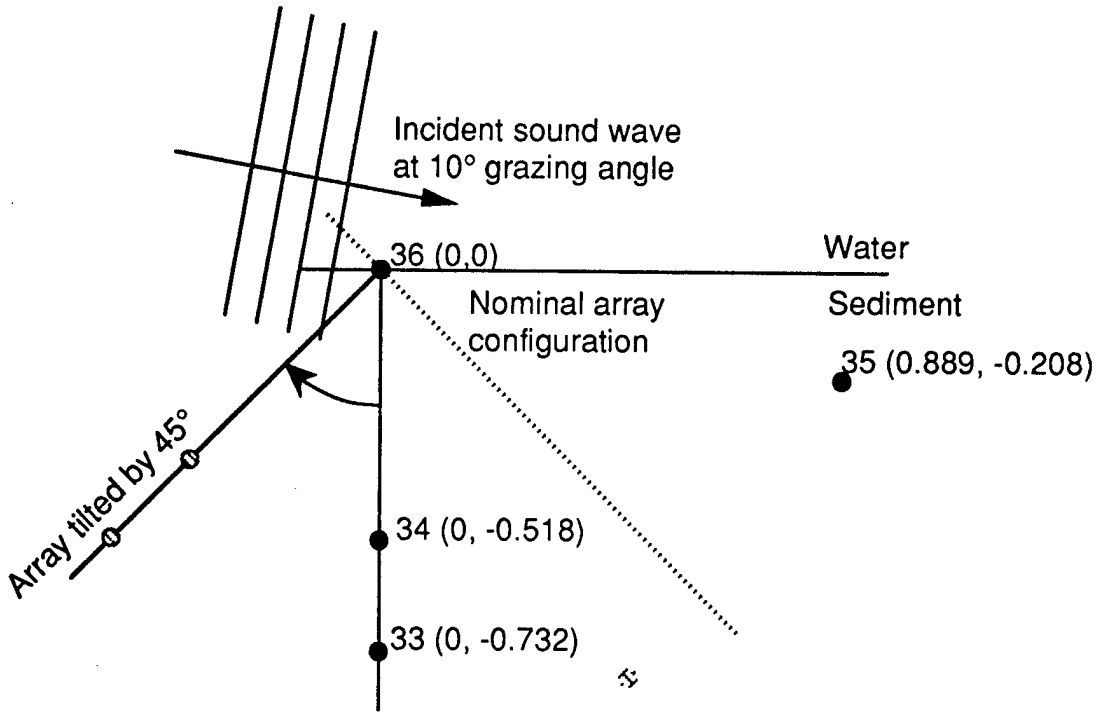

(b) Nominal array configuration and estimated array tilt angle

Figure 3.6
Muddy site, run 388, at a grazing angle of 10°.

ARL:UT
AS-95-635
NPC - rfg
9-95

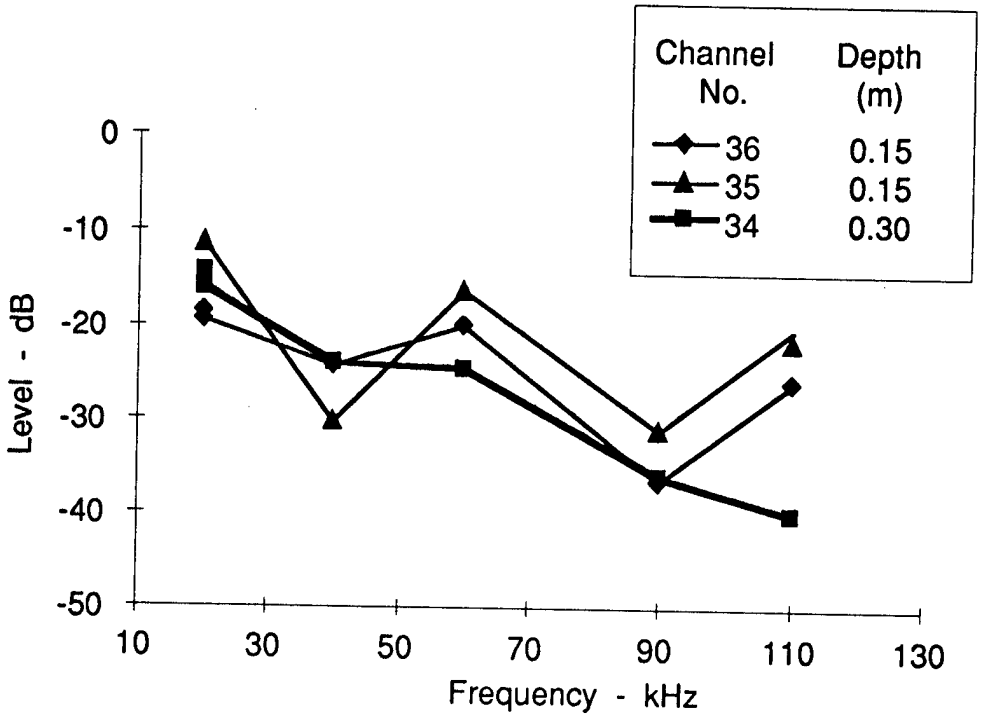

Figure 3.7
Signal levels in sandy sediment relative to the surface hydrophone as a function of frequency at a grazing angle of 30°.

ARL:UT
AS-95-636
NPC - rfg
9-95

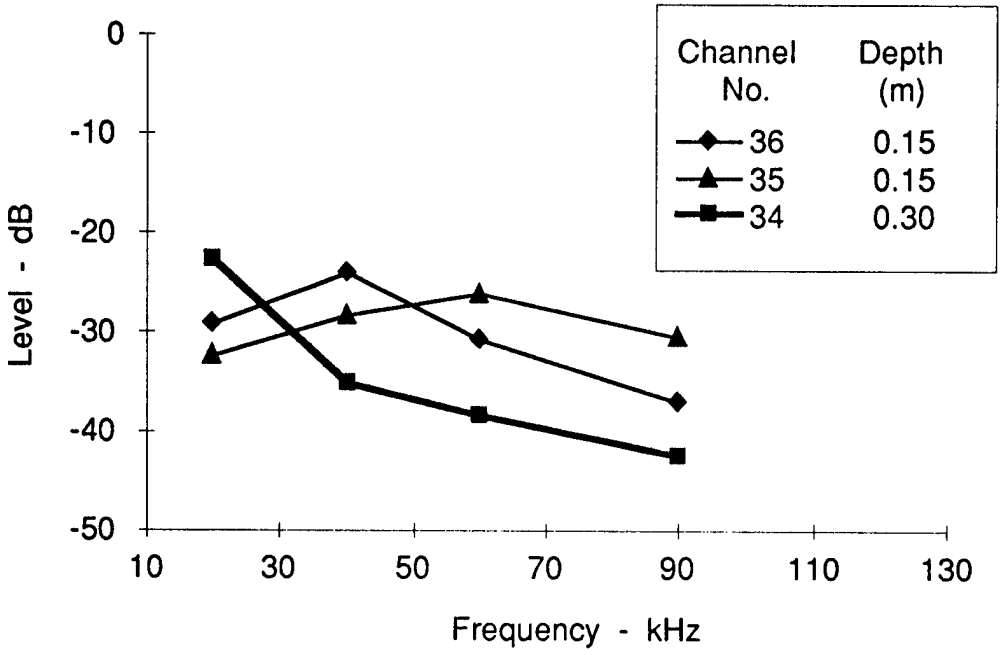

Figure 3.8
Signal levels in sandy sediment relative to the surface hydrophone as a function of frequency at a grazing angle of 10°.

ARL:UT
AS-95-637
NPC - rfg
9-95

Table 3.1
Estimated wave attenuation coefficients, in dB/m.

Sediment	Grazing angle (deg)	Speed (m/s)	Freq. (kHz) 20	Freq. (kHz) 40	Freq. (kHz) 60	Freq. (kHz) 90	Freq. (kHz) 110
Sand	30°	1700	-	-	24.7	-	-
Sand	30°	1200	-	-	-	-	90.8
Sand	10°	1200	-	27.8	26.7	18.6	-
Mud	10°	1400	-	-	-	2.2	9.0

The relative signal levels from the muddy site, at a grazing angle of 10° are shown in Fig. 3.9. At the lower frequencies, the signal at the deeper hydrophones appear to be stronger than those from the shallower hydrophones. As frequency is increased, the trend is gradually reversed and the signal levels behave more predictably, i.e., decreasing with depth. The differences at the lower frequencies are only a few decibels, and may be caused by calibration inaccuracies. Again, this makes it impossible to make reliable estimates of the attenuation coefficient, except perhaps at the highest frequencies. The results are shown in Table 3.1.

The values are consistent with previously reported values summarized by Hamilton.[2] The values from the sandy sediment fall near the top end of the reported range of values, while those from the muddy sediment fall near the bottom end. The attenuation in the mud is about ten times less than in the sand, which is consistent with measurements previously reported by Hamilton.[2]

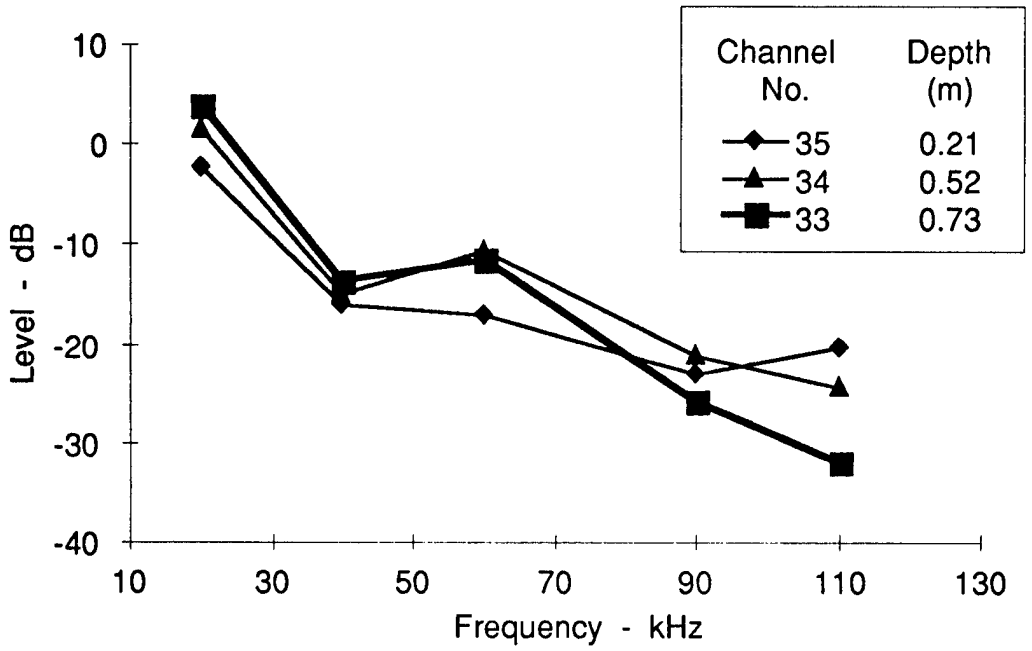

Figure 3.9
Signal levels in muddy sediment relative to the surface hydrophone as a function of frequency at a grazing angle of 10°.

ARL:UT
AS-95-638
NPC - rfg
9-95

This page intentionally left blank.

4. CONCLUSIONS

Acoustic data collected from buried hydrophones in ocean sediments, by NRL/SSC, were analyzed for direction, speed, and attenuation of sediment acoustic waves. The data were from two sites, a sandy site off Panama City, Florida, and a muddy site in Eckernförde, Germany. Acoustic pulses were transmitted from a projector in the water towards a hydrophone array buried in the sediment at a selection of discrete grazing angles.

In the sandy sediment, two acoustic waves were detected, one at a speed of 1700 m/s and the other at 1200 m/s, approximately. Both waves were present at a grazing angle of 30°, but only the slow wave was present at 10°. The signal levels did not decay monotonically with depth in the 30° case, possibly due to interference between the two waves, making it difficult to estimate the attenuation coefficient. At 10° the slow wave was dominant, and the signal levels were more consistent, although at 20 kHz the signal level at the deepest hydrophone was stronger than those at shallower depths. Calculations were made of the attenuation coefficients where signal levels decreased with depth in a monotonic manner. The results fall near the top end of the range of values reported for ocean sediments, and are consistent with values for sandy sediments.

In the muddy sediment, only one acoustic wave was detected, at a speed of approximately 1400 m/s. The signal levels appeared to increase with depth at the lower end of the frequency band, and to decrease with depth at the high end, with a gradual transition in between. Calibration inaccuracies are the most likely cause, since the differences at the lower frequencies were small – only a few decibels. Where the signal levels decrease with increasing depth, calculations were made of the attenuation coefficient. The values are consistent with previously reported values for muddy sediments, and are a factor of ten smaller than those of the sandy sediment.

This page intentionally left blank.

5. ACKNOWLEDGMENTS

This was a joint project between NRL/SSC and ARL:UT. The NRL/SSC team that collected the data was led by Dr. Steve Stanic. Supporting environmental data were collected by other participants in the CBBL SRP. There was excellent cooperation between all participants.

This page intentionally left blank.

REFERENCES

1. Kevin B. Briggs and Michael D. Richardson, "Geoacoustic and Physical Properties of Near Surface Sediments in Eckernförde Bay," Proceedings of the Gassy Mud Workshop, Kiel, Germany, 11-12 July 1994, pp. 39-46.

2. E. L. Hamilton, "Geoacoustic Modeling of the Sea Floor," J. Acoust. Soc. Am. 68, 1313-1340 (1980).

This page intentionally left blank.

20 April 1995

DISTRIBUTION LIST
ARL-TR-95-11
Final Report under Contract N00039-91-C-0082,
TD No. 01A2059, Analysis of Sea Test Data I

Copy No.

Commanding Officer
Naval Research Laboratory
Stennis Space Center, MS 39529-5004

1	Attn:	M. Richardson (Code 7431)
2		S. Tooma (Code 7130)
3		D. Ramsdale (Code 7170)
4		D. Young (Code 7331)
5		P. Fleischer (Code 7431)
6		K. Briggs (Code 7431)
7		P. Valent (Code 7401)
8		R. Love (Code 7174)
9		E. Franchi (Code 7100)
10		R. Meredith (Code 7174)
11		S. Stanic (Code 7174)
12 - 23		Library (Code 7032.2)

Office of Naval Research
Department of the Navy
Arlington, VA 22217-5000

24	Attn:	J. Kravitz (Code 322GG)
25		J. Simmen (Code 321OA)
26		E. Chaika (Code 322TE)
27		W. Ching (Code 321TS)
28		T. Goldsberry (Code 321W)
29		D. Houser (Code 333)

Commanding Officer
Naval Oceanographic Office
Stennis Space Center, MS 39522-5001

30	Attn:	J. Bunce (N31)
31		E. Beeson (N3)

Commanding Officer
Meteorological and Oceanic Command
Stennis Space Center, MS 32529

32	Attn:	D. Durham (N5A)
33		R. L. Martin (N5C)

Distribution List for ARL-TR-95-11 under Contract N00039-91-C-0082, TD No. 01A2059 (cont'd)

Copy No.

Commander
Naval Sea Systems Command
Department of the Navy
Washington, DC 20362-5101
34 Attn: J. Grembi (PMO407)
35 D. Gaarde (PMO407)

G & C Systems Manager
MK48/ADCAP Program Office
National Center 2
2521 Jefferson Davis Hwy.
12W32
Arlington, VA 22202
36 Attn: H. Grunin (PMO402E1)

Program Manager
MK50 Torpedo Program Office
Crystal Park 1
2011 Crystal Drive
Suite 1102
Arlington, VA 22202
37 Attn: A. Knobler (PMO406B)

Commander
Dahlgren Division
Naval Surface Warfare Center
Dahlgren, VA 22448-5001
38 Attn: Library

Commander
Dahlgren Division
Naval Surface Warfare Center
Silver Spring, MD 20903-5000
39 Attn: S. Martin (Code G94)
40 J. Sherman (Code N50)
41 M. Stripling (Code N04W)

Distribution List for ARL-TR-95-11 under Contract N00039-91-C-0082, TD No. 01A2059 (cont'd)

Copy No.

Commanding Officer
Coastal Systems Station, Dahlgren Division
Naval Surface Warfare Center
Panama City, FL 32407-5000

42 Attn: M. Hauser (Code 10CD)
43 R. Lim (Code 130B)
44 E. Linsenmeyer (Code 10P)
45 D. Todoroff (Code 130)

Commander
Naval Undersea Warfare Center Division
New London, CT 06320-5594

46 Attn: J. Chester (Code 3112)
47 P. Koenig (Code 33A)

Advanced Research Projects Agency
3701 North Fairfax Drive
Arlington, VA 22203-1714

48 Attn: W. Carey

Commander
Naval Undersea Warfare Center Division
Newport, RI 02841-5047

49 Attn: J. Kelly (Code 821)
50 F. Aidala (Code 842)
51 W. Gozdz (Code 843)

Officer in Charge
Arctic Submarine Laboratory
Naval Undersea Warfare Center
San Diego, CA 92152-5019

52 Attn: R. Anderson (Code 19)

Office of the Chief of Naval Operations
Department of the Navy
Washington, DC 20350-2000

53 Attn: R. Widmayer (N852T)
54 H. Montgomery (N911)
55 J. Boosman (N911D2)

Distribution List for ARL-TR-95-11 under Contract N00039-91-C-0082, TD No. 01A2059 (cont'd)

Copy No.

	Commander Mine Warfare Command 325 5th Street SE Corpus Christi, TX 78419
56	Attn: G. Pollitt (Code N02R)
	DTIC-OCC Defense Technical Information Center 8725 John J. Kingman Road, Suite 0944
57 - 68	Fort Belvoir, VA 22060-6218
	Applied Physics Laboratory The University of Washington 1013 NE 40th Street Seattle, WA 98105-6698
69	Attn: D. Jackson
70	S. Kargl
71	Library
	Applied Research Laboratory The Pennsylvania State University P. O. Box 30 State College, PA 16804-0030
72	Attn: R. Goodman
73	E. Liszka
74	D. McCammon
75	F. Symons
76	Library
	Presearch, Inc. 8500 Executive Park Avenue Fairfax, VA 22031
77 - 79	Attn: J. R. Blouin
	Ocean Engineering Department Massachusetts Institute of Technology 77 Massachusetts Avenue Cambridge, MA 02139
80	Attn: R. J. Fricke

Distribution List for ARL-TR-95-11 under Contract N00039-91-C-0082, TD No. 01A2059 (cont'd)

Copy No.

	Physics Department The University of Texas at Austin Austin, TX 78712
81	Attn: W. D. McCormick
82	M. Fink
83	T. Griffy
	Aerospace Engineering Department The University of Texas at Austin Austin, TX 78712
84	Attn: M. Stern
85	Robert A. Altenburg, ARL:UT
86	Hollis Boehme, ARL:UT
87	Frank A. Boyle, ARL:UT
88	Nicholas P. Chotiros, ARL:UT
89	John M. Huckabay, ARL:UT
90	Thomas G. Muir, ARL:UT
91	Library, ARL:UT
92 - 98	Reserve, ARL:UT